J Mater Sci (2009) 44:3098–3111
DOI 10.1007/s10853-009-3412-0

On the acid–base stability of Keggin Al_{13} and Al_{30} polymers in polyaluminum coagulants

Zhaoyang Chen · Zhaokun Luan · Zhiping Jia · Xiaosen Li

Received: 29 July 2008 / Accepted: 17 March 2009 / Published online: 7 April 2009

Abstract The acid–base stabilities of Al_{13} and Al_{30} in polyaluminum coagulants during aging and after dosing into water were studied systematically using batch and flow-through acid–base titration experiments. The acid decomposition rates of both Al_{13} and Al_{30} increase rapidly with the decrease in solution pH. The acid decompositions of Al_{13} and Al_{30} with respect to H^+ concentration are composed of two parallel first-order and second-order reactions, and the reaction orders are 1.169 and 1.005, respectively. The acid decomposition rates of Al_{13} and Al_{30} increase slightly when the temperature increases from 20 to *ca.* 35 °C, but decrease when the temperature increases further. Al_{30} is more stable than Al_{13} in acidic solution, and the stability difference increases as the pH decreases. Al_{30} is more possible to become the dominant species in polyaluminum coagulants than Al_{13}. The acid catalyzed decomposition and followed by recrystallization to form bayerite is one of the main processes that are responsible for the decrease of Al_{13} and Al_{30} in polyaluminum coagulants during storage. The deprotonation and polymerization of Al_{13} and Al_{30} depend on solution pH. The hydrolysis products are positively charged, and consist mainly of repeated Al_{13} and Al_{30} units rather than amorphous $Al(OH)_3$ precipitates. Al_{30} is less stable than Al_{13} upon alkaline hydrolysis. Al_{13} is stable at pH < 5.9, while Al_{30} lose one proton at the pH 4.6–5.75. Al_{13} and Al_{30} lose respective 5 and 10 protons and form $[Al_{13}]_n$ and $[Al_{30}]_n$ clusters within the pH region of 5.9–6.25 and 5.75–6.65, respectively. This indicates that Al_{30} is easier to aggregate than Al_{13} at the acidic side, but $[Al_{13}]_n$ is much easier to convert to $Al_{sol-gel}$ than $[Al_{30}]_n$. Al_{30} possesses better characteristics than Al_{13} when used as coagulant because the hydrolysis products of Al_{30} possess higher charges than that of Al_{13}, and $[Al_{30}]_n$ clusters exist within a wider pH range.

Z. Chen (✉) · X. Li (✉)
Key Laboratory of Renewable Energy and Gas Hydrate, CAS, Guangzhou Institute of Energy Conversion, Chinese Academy of Sciences, 510640 Guangzhou, China
e-mail: chenzy@ms.giec.ac.cn

X. Li
e-mail: lixs@ms.giec.ac.cn

Z. Luan · Z. Jia
State Key Laboratory of Environmental Aquatic Chemistry, Research Center for Eco-Environmental Sciences, Chinese Academy of Sciences, 100085 Beijing, China

Introduction

The aqueous chemistry of hydrolytic polymeric aluminum (HPA) solutions has been extensively investigated during the last 40 years [1–3]. Al polycation species in HPA solutions were widely used and studied in water treatment, material science, pharmaceutical, geochemistry, environmental science, bio-toxicology, etc. [4–14]. A series of hydrolysis species formed in HPA solutions depends on various factors, such as Al concentration, degree of basification, reaction temperature and time, type of base, rate and style for base addition and coexisting anions [15, 16]. In spite of a great deal of literatures, the chemical speciation in HPA solutions has not been completely determined yet due to the complexity of the solution [17]. Until now, only 10 Al species have been clearly characterized and identified in HPA solutions. These species include: five monomers Al^{3+}, $Al(OH)^{2+}$, $Al(OH)_2^+$, $Al(OH)_3$ (aq), and $Al(OH)_4^-$; dimer $[Al_2(OH)_2]^{4+}$; two Keggin polymers $[AlO_4Al_{12}(OH)_{24}(H_2O)_{12}]^{7+}$ (ε-Al_{13}) and $[Al_{30}O_8(OH)_{56}(H_2O)_{24}]^{18+}$ (δ-Al_{30}) [2, 18, 19]; and two flat polymers

$[Al_{13}(OH)_{24}(H_2O)_{24}]^{15+}$ and $[Al_8(OH)_{14}(H_2O)_{18}]^{10+}$ [20, 21].

Among these Al species, the Keggin ε-Al_{13} polycation received the most extensive attention in previous investigations due to its ubiquity and high charges. The Keggin Al_{30} species was the largest Al polycation that was identified in HPA solutions, and its structure was characterized by Allouche et al. and Rowsell et al. using in situ ^{27}Al nuclear magnetic resonance (NMR) and single crystal X-ray diffraction [18, 19]. Al_{30} species consists of two δ-Al_{13} Keggin units connected by a crown made of four hexa-coordinated Al atoms (AlO_6), and it can be prepared by thermal treatment of the HPA solutions containing ε-Al_{13} precursor [18]. The giant Al_{30} species possesses 18 positive charges and is approximately 2 nm in length [22]. Due to its unique molecular structure, nanometer dimension and high positive charges, Al_{30} has received extensive attentions from many fields since it was identified. The research contents concerned on the preparing methods and mechanism, structural characteristics, chemical property, etc. [23–29].

In the field of water treatment, the pre-hydrolyzed polyaluminum coagulants are the most widely used coagulants and receive extensive research [4]. It is generally believed that Al_{13} is the optimal species for coagulation in polyaluminum coagulant due to its high charge neutralization capability, strong structure stability, and nanometer molecular dimension [30]. However, the commercial polyaluminum coagulant contained only small amount of Al_{13} due to the transformation of Al_{13} to high polymers in highly concentrated HPA solutions [31]. Compared with Al_{13}, Al_{30} achieved better turbidity removal within a broader dosage range and a wider pH region due to its high charge neutralization capacity and good flocs formation capacity [27]. Furthermore, Al_{13} tends to convert to Al_{30} species, when the high concentrated HPA solutions were subjected to thermal treatment [28, 32]. The formation conditions of Al_{30} are consistent with the preparation process of commercial polyaluminum coagulants. High temperature and long-term thermal treatment are inevitably needed during the preparation of commercial polyaluminum coagulants, and high Al concentration is absolutely necessary when application cost is considered. So Al_{30} as a high active species is very significant to water treatment flocculation.

It is not practical to prepare fresh coagulant for field usage in water treatment. For a commercial coagulant, acid stability is needed for storing purposes. Because the polymeric Al species in polyaluminum coagulants are exposed to medium and high acidic environment, the acid-catalyzed decomposition of Al_{13} and Al_{30} may be one of the main reasons that result in the decrease of Al_{13} and Al_{30} in polyaluminum coagulants during storing. Al_{13} in polyaluminum coagulants was dissociated to Al monomers (Al_m) and Al oligomers (Al_{olig}) by H^+, and these Al_m and Al_{olig} re-crystallized to form bayerite [28]. Furrer et al. [33] studied the proton-promoted decomposition of Al_{13} using batch and flow-through acid titration experiments, but their studies were aimed at aquatic geochemistry, and linked weathering and acidic dissolution of Al-bearing minerals. The total Al concentration (Al_T) of Al_{13} containing solutions employed for their acid titration were lower than 5 mM, which was much lower than that of polyaluminum coagulants ($Al_T \geq 0.2$ M). The concentration of H^+ in polyaluminum coagulants is much higher than that in surface water and soil chemistry, so the decomposition behavior of Al_{13} and Al_{30} in polyaluminum coagulants should be different from that occurred in geochemistry. However, there is a lack of investigation on acid decomposition of Al_{13} and Al_{30} in solutions with Al_T as in polyaluminum coagulants.

Furthermore, the coagulation performance of polyaluminum coagulants is not only related to Al species distribution, but also closely related to Al species hydrolysis, aggregation and precipitation after dosing into water. In fact, the coagulants dosing process is similar to dilution and alkalization of coagulants simultaneously. The alkaline hydrolysis after coagulants dosing into water is very important to flocculation efficiency, and which is dependent on the acid–base property of Al species and the chemical composition of solution. Furrer et al. [34] studied the acid–base properties of Al_{13} using batch and flow-through base titration of aqueous solutions containing 0.01–1 mM of Al_{13}. Lee et al. [35] studied the acid–base chemistry of Keggin Al_{13}, $GeAl_{12}$, and $GaAl_{12}$ using base titration, and the results indicated that $GeAl_{12}$ was the most acidic, followed by Al_{13} and $GaAl_{12}$. Rustad examined the relative Brønsted acidities of the functional groups on Al_{13} and Al_{30} using molecular dynamics simulation, and revealed that Al_{30} was more acidic than Al_{13} due to the presence of acidic η-H_2O functional groups [29]. However, the above base titration investigations were also carried out in solution with very low Al_T, and aimed at the field of aqueous geochemistry. Although titration of polyaluminum solutions with low Al_T can avoid the aggregation of Al species, reduce the diffusion barrier of OH^- and ensure the accurate pH measurement, the polymerization and aggregation of Al_{13} and Al_{30} during coagulation is inevitable but is absolutely necessary for the work of flocs absorption and sweeping flocculation. A medium concentrated polyaluminum solution (0.05–0.2 M) is more practical than a low concentrated polyaluminum solution when using base titration method to study the stability and species transformation of Al_{13} and Al_{30} in polyaluminum coagulants after dosing into water.

In this work, the acid decomposition kinetic of Al_{13} and Al_{30} in polyaluminum coagulants during storing was studied using batch and flow through acid titration experiments. The deprotonation reaction and aggregation behavior of

Al_{13} and Al_{30} species after dosing into water were studied by base titration. The research will help to elucidate the transformation mechanism of Al_{13} and Al_{30} in polyaluminum solutions, and to understand the hydrolysis/precipitation behavior and coagulation mechanism of Al_{13} and Al_{30}. The results will provide theoretic framework for the development of coagulants with high selectivity of Al_{13} or Al_{30}.

Materials and methods

Materials

The reagents used in this research work were all of analytical grade. All solutions were prepared using deionised water. Two coagulants containing high content of Al_{13} (abr. PAC_{Al13}) and Al_{30} (abr. PAC_{Al30}) were prepared by slowly neutralizing 1.0 M $AlCl_3$ solution with 0.6 M NaOH solution at 80 °C until Al hydrolysis ratio B ($B = [OH]/[Al]$) reached 2.4, and PAC_{Al30} was prepared by heating PAC_{Al13} at 95 °C for 12 h after PAC_{Al13} prepared.

The two coagulants were rested at 25 °C for 5 days before analysis, characterization, and titration experiments. Al_T was measured by inductively coupled plasma-atomic emission spectroscopy (Vista-MPX ICP-AES, Varian), and B was measured by chemical analysis according to the Chinese standard method (GB 15892-1995). The solution pH was measured using a pH meter (Orion 710A). The Al species distributions in these two coagulants were determined by Al-Ferron time-developed complex colorimetry on UV–vis spectrophotometer (DR/4000U, Hach) and by high-field ^{27}Al NMR method on Fast Fourier Transformation spectrometer (JNM-ECA600, JEOL). Based on the difference of the dissociation and complex reaction kinetic rate between Ferron and Al species, Al species in coagulants were divided into three types: monomeric species (Al_a) (reaction with Ferron within 1 min), planar oligomeric and medium polymeric species (Al_b) (reaction with Ferron from 1 to 120 min), and three-dimensional species or sol–gels (Al_c) (reaction with Ferron after 120 min or non-reaction with Ferron). Al_c was obtained by Al_T minus Al_a and Al_b [36]. In ^{27}Al NMR analysis, the species at 0 ppm was assigned to Al_m. The Al concentration for 62.5 and 70 ppm signals were multiplied by 13 and 15, respectively. This is to obtain the concentration of Al_{13} and Al_{30}, respectively. Al species that cannot be clearly measured (Al_u) was calculated by Al_T minus Al_m, Al_{13}, and Al_{30} [37]. The detailed preparation and characterization methods can be referred from our previous reports [27, 37]. The detailed specifications of these two coagulants used in this work are listed in Table 1.

Batch experiments on acid decomposition

A measured amount of PAC_{Al30} was added into a 100 mL conical bottle under stirring with a magnetic stirrer. The solution temperature was controlled using a thermostat water bath. A calculated amount of hydrochloric acid of predetermined concentration (0.1 M or 0.5 M) was added into the PAC_{Al30} solution under vigorous stirring. The pH values of the solution were recorded every 10 s using an automatic titrator (716 DMS Titrino, Metrohm Co.) until the pH became stable. The amount of hydrochloric acid added was equivalent to the amount of OH^- used during the preparation of PAC_{Al30}, and which could decompose all polymeric Al species into Al^{3+} theoretically. The acid decomposition experiments of PAC_{Al13} were conducted using the same method as described.

Flow-through experiments on acid decomposition

A flow-through experimental method reported by Furrer et al. [33] was adopted to study the acid decomposition kinetics of Al_{13} and A_{l30}. A 0.1 M PAC_{Al30} (diluent of 0.2 M PAC_{Al30}) was added into a 150 mL Erlenmeyer flask with an overflow ports until overflowing. The solution temperature in the Erlenmeyer flask was controlled using a thermostat water bath. Another solution of 0.1 M PAC_{Al30} was added to the flask together with a hydrochloric acid solution (HCl) of certain concentration. Separate peristaltic pumps were used to add these solutions into the overflowed flask at constant flow rate. The solutions were mixed vigorously using a magnetic stirrer. A constant solution volume was maintained in the flask by removing excessive solution through overflow ports. At the same time, the solution pH in the flask was recorded every 10 s using an automatic titrator (716 DMS Titrino, Metrohm Co.) until the pH reached a stable value. The experiment was later

Table 1 Al species distribution and pH values of coagulants used in this work

Samples		Al_T (M)	B	Al species distribution (%)							pH
Coagulants	Aging time			Al_a	Al_b	Al_c	Al_m	Al_{13}	Al_{30}	Al_u	
PAC_{Al13}	5 days	0.2	2.4	4.7	78.8	16.5	4.7	81.5	0.0	13.8	4.26
PAC_{Al30}	5 days	0.2	2.4	2.7	23.0	74.3	3.7	16.5	76.8	3.1	4.20

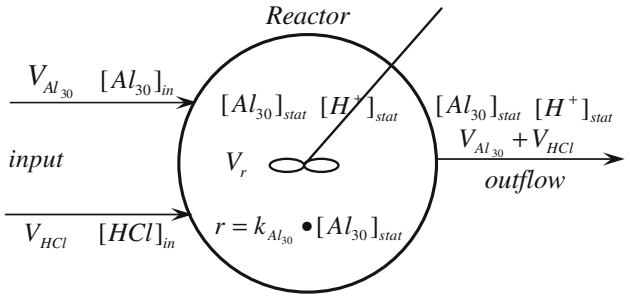

Fig. 1 The schematic flow sheet of the flow-through experiments

repeated by varying the concentration and flow rate of HCl. The pH electrode with automatic temperature compensation was calibrated by the three-point method.

The schematic flow sheet of the flow-through experiment is shown in Fig. 1. The experimental equipment was similar to a continuous flow reaction system. When the flow rate of feeding and concentration of PAC_{Al30} and hydrochloric acid, as well as the temperature in the reactor, maintained invariant, the system would ultimately reach a stable state. The concentrations of Al_{30} and H^+ in the reactor ($[Al_{30}]_{stat}$ and $[H^+]_{stat}$) would remain constant at the stable state. $[Al_{30}]_{stat}$ and $[H^+]_{stat}$, and the apparent rate coefficient ($k_{Al_{30}}$) and half-life ($t_{1/2}$) of Al_{30} acid decomposition reaction were then calculated according to the derivation in Appendix. The same methods were used for the kinetic study of acid decomposition of Al_{13}.

Base titration experiments on deprotonation and aggregation

Fifty milliliter PAC_{Al30} with a concentration of 0.1 M was added into a conical flask on an automatic titrator (716 DMS Titrino, Metrohm Co.) under stirring. The solution temperature was controlled by a thermostat water bath. A 0.02 M NaOH aqueous solution was added into the flask at a constant flow rate using a peristaltic pump until the solution pH reached above 10. The pH of the solution in the flask was recorded every 10 s using the automatic titrator. According to the equilibrium of OH^-, a dimensionless variable Z, defined by Furrer et al. [34], was adopted to represent the extent of deprotonation relative to the fully charged Keggin Al_{13}^{7+} or Al_{30}^{18+} species. And Z was calculated according to Eq. 1,

$$Z = \frac{30V_{\mathrm{NaOH}} \cdot C_{\mathrm{NaOH}} + 30(V_0 + V_{\mathrm{NaOH}}) \cdot ([\mathrm{H}^+] - [\mathrm{OH}^-])}{V_0 \cdot \mathrm{Al}_T}. \quad (1)$$

where V_{NaOH} and C_{NaOH} are the volume and concentration of the base added (mL and M, respectively). V_0 is the initial coagulant volume added into the flask (mL). $[H^+]$ and $[OH^-]$ are the respective concentrations of H^+ and OH^- in the solution, and which can be calculated from the solution pH (M). The same base titration procedure and data processing methods were employed to study the deprotonation and aggregation of Al_{13}.

Results and discussion

Acid decomposition of Al_{13} and Al_{30}

As Al_{13} possessed very good stability under acidic conditions and met the requirements of commercialization [16], Al_{13} was used as a reference to study the acid stability of Al_{30} in this investigation. The pH developments of PAC_{Al13} and PAC_{Al30} after mixing with equivalent hydrochloric acid are displayed in Fig. 2. The effect of using 0.1 and 0.5 M hydrochloric acid are shown in Fig. 2a and b, respectively. The pH of PAC_{Al13} and PAC_{Al30} decreased sharply initially after hydrochloric acid addition, and then

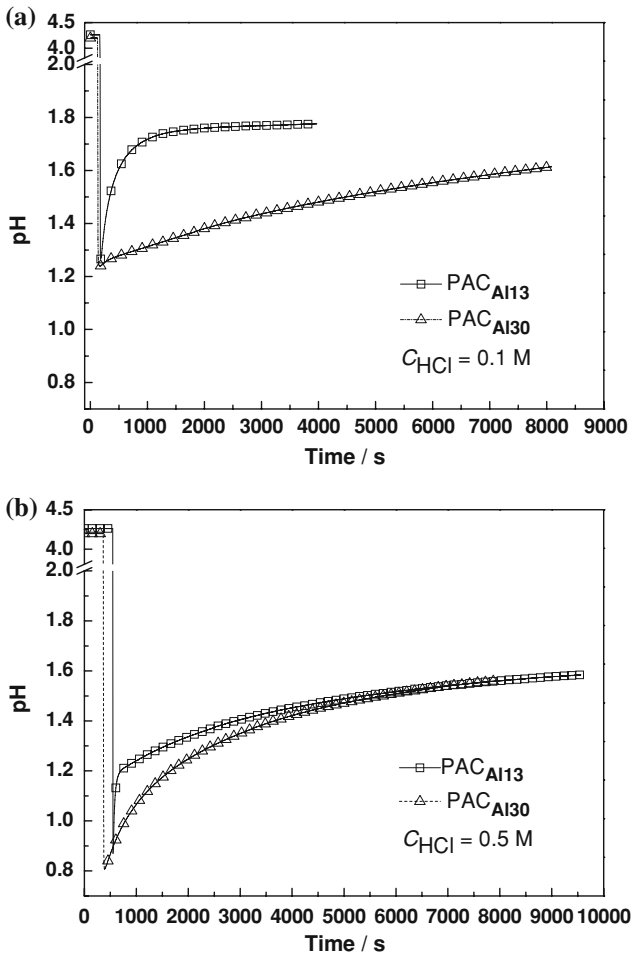

Fig. 2 The pH development of PAC_{Al13} and PAC_{Al30} after mixing with equivalent hydrochloric acid. **a** 0.1 M hydrochloric acid used and **b** 0.5 M hydrochloric acid used

rose up. The rate of pH increase, however, depended on the coagulant and the concentration of the hydrochloric acid. The pH of PAC_{Al13} rose up rapidly first, then rose slowly, and leveled off at last, but the pH of PAC_{Al30} increased slowly during the whole period, and its pH was lower than that of PAC_{Al13}. This indicated that Al_{30} in PAC_{Al30} was more stable than Al_{13} in PAC_{Al13} when exposed to acid environment. During the acid decomposition experiments, Al_{13} and Al_{30} in PAC_{Al13} and PAC_{Al30} were acting as Lewis alkali, and reacted with H^+ in solution. The acid–base neutralization caused the dissociation of hydroxyl bridge bond in Al_{13} and Al_{30}, and which resulted in the decomposition of these polymeric Al species. The neutralization reaction consumed free H^+ in solution and resulted in pH rise. The faster the pH increased, the faster the polymeric Al species decomposed, and the less stable the polymeric Al species was.

Compared Fig. 2a with b, we can see that the acid decomposition rates of PAC_{Al30} and PAC_{Al13} depend on the solution pH. The differences in the stability of Al_{13} and Al_{30} species increased when low concentration of hydrochloric acid (0.1 M) was used. When 0.5 M hydrochloric acid was used, the pH of the two coagulants reached the same value finally, and both Al_{13} and Al_{30} were completely dissociated into Al^{3+} by H^+ due to the very low solution pH.

The typical pH curves of PAC_{Al13} and PAC_{Al30} during flow-through experiments are shown in Fig. 3. The pH decreased drastically at the beginning of reaction, and then decreased slowly before reaching steady state. The steady state was considered to be reached when the change of the solution pH did not exceed 0.005 pH unit within 30 min in the experiments. Corresponding to the decrease of pH, the acid decomposition rate of Al_{13} and Al_{30} in the reactor increased rapidly first, and then increased slowly until a dynamic equilibrium is reached. The concentrations of Al_{13} or Al_{30} in the reactor remain constant at the steady state.

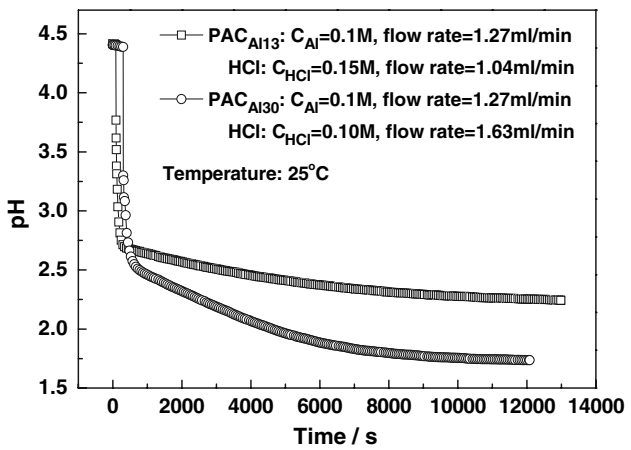

Fig. 3 The typical pH trajectory of PAC_{Al13} and PAC_{Al30} during flow-through experiments

The volume of the reactor was 135 mL. The mean residence time of reactants in the reactor depended on the volume flow rate of inflows, and it was about 2,500–3,500 s. The steady state, therefore, can be achieved within three to five times of the mean residence time. The results of flow-through experiments on the acid decomposition of Al_{13} and Al_{30} are summarized in Tables 2 and 3, respectively.

Effect of pH on the decomposition of Al_{13} and Al_{30}

The rate constants of acid decomposition of Al_{13} and Al_{30} as a function of pH at 25 °C are shown in Fig. 4. As can be seen from Fig. 4a, the acid decomposition rate constants increased rapidly when the pH decreased from 3.7 to 1.7, which indicated that the acid stability of Al_{13} and Al_{30} depends significantly on solution pH. The logarithm of the rate constants (log k) and pH exhibited a good linear correlation, and the slopes of log k versus pH were –1.169 and –1.005 for Al_{13} and Al_{30}, respectively (Fig. 4b). These slopes for Al_{13} and Al_{30} were between 1.0 and 2.0, which indicated that more than one proton was involved in the rate limiting steps. The reaction order with respect to the free proton concentration exceeded 1, and it was between first-order and second-order reactions. Two parallel reaction processes were considered involved in the decomposition of Al_{13} and Al_{30}, i.e., a first-order and a second-order reactions

$$r_{Al13} = r_1 + r_2 = k_1 \cdot [H^+] \cdot [Al_{13}] + k_2 \cdot [H^+]^2 \cdot [Al_{13}] \quad (2)$$

and

$$r_{Al30} = r_1 + r_2 = k_1 \cdot [H^+] \cdot [Al_{30}] + k_2 \cdot [H^+]^2 \cdot [Al_{30}]. \quad (3)$$

In comparing the results of acid decomposition of PAC_{Al13} and PAC_{Al30} in Tables 2 and 3, the pH of PAC_{Al13} at steady state was higher than that of PAC_{Al30}, and at the same time, the apparent rate constants of acid decomposition of Al_{13} (k_{Al13}) were higher than that of Al_{30} (k_{Al30}) under the same pH and temperature conditions. This shows that the acid stability of Al_{30} was higher than that of Al_{13}. Since the difference between k_{Al13} and k_{Al30} increased with the decrease in pH, the stability difference between Al_{30} and Al_{13} enlarged as pH reduced. The slope of log k versus pH of PAC_{Al13} (–1.169) is smaller than that of PAC_{Al30} (–1.005), indicating that the second-order reaction contributed more to the acid decomposition of PAC_{Al13} than to PAC_{Al30}. The second-order reaction also resulted in the much more rapid decomposition of Al_{13} than Al_{30} in low pH solution (pH $\leq$ 3.0).

As can be seen from Tables 2 and 3, the half-life of pseudo-first-order reaction of Al_{30} and Al_{13} increased rapidly with the increase in pH. The half-life of Al_{13} increased from 48 to 2,076 min when the pH of PAC_{Al13}

Table 2 The experimental conditions and results of flow-through experiments on PAC_{Al13}

PAC_{Al13}		Hydrochloric acid		Temp. (°C)	pH at stable state	k_{Al13} (min^{-1})	LN(k_{Al13})	$[Al_{13}]_{stat}$ (M)	Half-life (min)
$C_{PACAl13}$ (M)	Flow rate (mL/min)	C_{HCl} (M)	Flow rate (mL/min)						
0.1	1.56	0.1000	1.60	20	2.231	0.013648	−4.29413	0.031187	51
0.1	1.56	0.1000	1.60	30	2.338	0.014278	−4.24901	0.030667	49
0.1	1.56	0.1000	1.60	35	2.274	0.013918	−4.27459	0.030953	50
0.1	1.56	0.1000	1.60	40	2.261	0.013839	−4.28028	0.031031	50
0.1	1.73	0.1000	1.35	25	2.460	0.009407	−4.66634	0.039767	74
0.1	1.56	0.0500	1.60	30	2.823	0.005705	−5.16642	0.039689	121
0.1	1.56	0.0500	1.60	36	2.798	0.005678	−5.17108	0.039728	122
0.1	1.56	0.0500	1.60	39	2.779	0.005657	−5.17481	0.039754	123
0.1	1.56	0.0500	0.753	26	3.116	0.001766	−6.33912	0.061139	393
0.1	1.56	0.0500	0.753	30	3.082	0.001758	−6.34356	0.061165	394
0.1	1.56	0.0500	0.753	35	3.175	0.001778	−6.33223	0.0611	390
0.1	1.56	0.0500	0.753	40	3.151	0.001773	−6.33491	0.061113	391
0.1	1.27	0.0500	1.040	20	2.750	0.003096	−5.77776	0.046553	224
0.1	1.27	0.0500	1.040	25	2.780	0.003117	−5.77102	0.046514	222
0.1	1.27	0.0500	1.040	30	2.793	0.003125	−5.76824	0.046488	222
0.1	1.27	0.0500	1.040	38	2.803	0.003130	−5.76679	0.046475	221
0.1	1.27	0.0063	1.040	25	3.651	0.000334	−8.00458	0.053924	2076
0.1	1.27	0.0125	1.040	25	3.367	0.000681	−7.29189	0.052871	1018
0.1	1.27	0.0250	1.040	25	3.070	0.001425	−6.55354	0.050752	486
0.1	1.27	0.0385	1.040	25	2.927	0.002317	−6.06737	0.048425	299
0.1	1.27	0.0500	1.040	25	2.780	0.003117	−5.77102	0.046514	222
0.1	1.27	0.0774	1.040	25	2.608	0.005383	−5.22453	0.041821	129
0.1	1.73	0.1000	1.350	25	2.460	0.007910	−4.83963	0.041704	88
0.1	1.56	0.1000	1.350	25	2.303	0.012200	−4.40632	0.034229	57
0.1	1.27	0.1500	1.040	25	2.243	0.014389	−4.24131	0.029861	48

$C_{PACAl13}$ is the concentration of PAC_{Al13} calculated by Al

C_{HCl} is the concentration of hydrochloric acid

$[Al_{13}]_{stat}$ is the concentration of Al_{13} at steady state calculated by Al

increased from 2.243 to 3.651 at 25 °C (Table 2). However, the half-life of Al_{30} increased from 57 to 4,359 min when the pH increased from 1.74 to 3.62 at 25 °C (Table 3). For polyaluminum coagulants with $Al_T = 1.0$–2.5 M, $B = 2.4$, the pH of the coagulants ranged from 1.0 to 3.6, and the half-life of Al_{13} and Al_{30} under such pH condition were about 100–2,000 min and 270–4,500 min, respectively. Furthermore, the acid decomposition accelerated because the coagulant preparation temperature was higher than 25 °C. So the acid decomposition of Al_{13} and Al_{30} is one of the main reasons that result in the low content of Al_{13} and Al_{30} in commercial coagulants. The half-life of Al_{30} was twice longer than that of Al_{13}. So Al_{30} is more likely to become the dominant species in polyaluminum coagulants than Al_{13}.

The decomposition rate measured in this investigation was higher than the results obtained in our previous report because the concentration of Al_{13} and Al_{30} in current flow-through experiments (*ca.* 0.05 M) was lower than the Al concentration in our previous studies [27]. The possible reasons for the low decomposition rate in high concentrated polyaluminum coagulant included: (1) the transition-state or protonated precursor of Al_{13} or Al_{30} would re-polymerize to form Al_{13} and Al_{30} species rather than decompose into Al^{3+} completely under high Al concentration. (2) There existed other Al species whose alkalinity was higher than that of Al_{13} and Al_{30} species, and these species inhibited the decomposition of Al_{13} and Al_{30}, i.e., H^+ in solution tended to react with these Al species with high alkalinity. (3) There was some Al species in polyaluminum coagulant, which was composed of aggregates of Al_{13} or Al_{30}, and was classified as Al_u (^{27}Al NMR method) or Al_c (Al-Ferron method) species. Protonation of these aggregates of Al_{13} or Al_{30} caused the dissociation of

Table 3 The experimental conditions and results of flow-through experiments on PAC_{Al30}

PAC_{Al30}		Hydrocloric acid		Temp. (°C)	pH at stable state	k_{Al30} (min^{-1})	LN(k_{Al30})	$[Al_{30}]_{stat}$ (M)	Half-life (min)
$C_{PACAl30}$ (M)	Flow rate (mL/min)	C_{HCl} (M)	Flow rate (mL/min)						
0.1	1.27	0.1	1.63	20	1.61	0.009260	−4.68203	0.0306	75
0.1	1.27	0.1	1.63	25	1.74	0.012170	−4.40881	0.0279	57
0.1	1.27	0.1	1.63	30	1.76	0.012586	−4.37521	0.0276	55
0.1	1.27	0.1	1.63	38	1.66	0.010420	−4.56406	0.0294	67
0.1	1.27	0.1	1.04	38	2.10	0.006688	−5.00750	0.0396	104
0.1	1.27	0.1	1.63	25	1.74	0.012170	−4.40881	0.0279	57
0.1	1.27	0.1	1.04	25	1.975	0.006041	−5.10917	0.0405	115
0.1	1.27	0.0736	1.04	25	2.175	0.004285	−5.45252	0.0441	162
0.1	1.27	0.05	1.04	25	2.40	0.002796	−5.87973	0.0474	248
0.1	1.27	0.0348	1.04	25	2.534	0.001832	−6.30218	0.0498	378
0.1	1.27	0.025	1.04	25	2.68	0.001277	−6.66292	0.0513	543
0.1	1.27	0.0125	1.04	25	2.99	0.000619	−7.38790	0.0531	1120
0.1	1.27	0.0063	1.04	25	3.306	0.000306	−8.09133	0.054	2264
0.1	1.27	0.0031	1.04	25	3.62	0.000153	−8.78708	0.0546	4539

$C_{PACAl30}$ denotes the concentration of PAC_{Al30} calculated by Al

C_{HCl} is the concentration of hydrochloric acid

$[Al_{30}]_{stat}$ denotes the concentration of Al_{30} under steady state calculated by Al

hydroxyl-bridge between Al_{13} and Al_{30} units, and which resulted in the formation of Al_{13} and Al_{30}.

Effect of temperature on the decomposition of Al_{13} and Al_{30}

In Tables 2 and 3, both the steady-state pH values and the apparent rate constants increased slightly with the increase in temperature for PAC_{Al13} and PAC_{Al30} when the temperature was lower than 35 °C. When the temperature rose above 35 °C, the steady-state pH decreased slightly instead, and the apparent rate constants also decreased slightly. The effect of temperature on the apparent rate constant of acid decomposition of the two coagulants was less important than the solution pH in 20–40 °C. The acid decomposition of Al_{13} and Al_{30} at temperature higher than 40 °C was not studied due to the temperature limitation of the pH electrode. The acid decomposition of Al_{13} and Al_{30} contain two parallel processes: first-order and second-order reactions. The first-order reaction is exothermic, and the second-order reaction is endothermic [33]. When the reaction temperature rose, the first-order reaction was suppressed, and the second-order reaction was accelerated. The apparent rate constant is dependent on the combination of the two parallel reactions, which may be why the apparent rate constant of acid decomposition of Al_{13} and Al_{30} decreased with the increase in temperature when the temperature increases above *ca.* 35 °C in this research.

As can be seen from Tables 2 and 3, under the same condition, the steady-state concentrations $[Al_{13}]_{stat}$ and $[Al_{30}]_{stat}$ changed very slightly with the changing temperature. However, $[Al_{13}]_{stat}$ and $[Al_{30}]_{stat}$ increased with the increase in pH, which indicated that there exist a good chemical equilibrium between H^+ and polyaluminum species. $[Al_{30}]_{stat}$ was higher than $[Al_{13}]_{stat}$ under the same condition, which further verified that Al_{30} was more stable than Al_{13} under acid condition.

Alkaline aggregation of Al_{13} and Al_{30}

The deprotonation and aggregation of Al_{13} and Al_{30} during flocculation process were modeled by base titration using an automatic titrator. The variations of pH as a function of titration time and theoretical OH/Al (OH^-added during coagulant preparation and titration divide by Al concentration in solution) are displayed in Fig. 5. The calculated deprotonation number, *Z*, as a function of pH for PAC_{Al13} and PAC_{Al30} are shown in Fig. 6. There were eight characteristic points on the base titration curves of PAC_{Al13} or PAC_{Al30}: four critical points and four inflection points (Fig. 5b). Correspondingly, there also existed eight characteristic points on the calculated deprotonation curves in Fig. 6. The four critical points were the crossing points of two neighboring tangent lines passing through the inflection points, and the four inflection points (α, β, γ, and θ) were the points where the value of the second derivative of

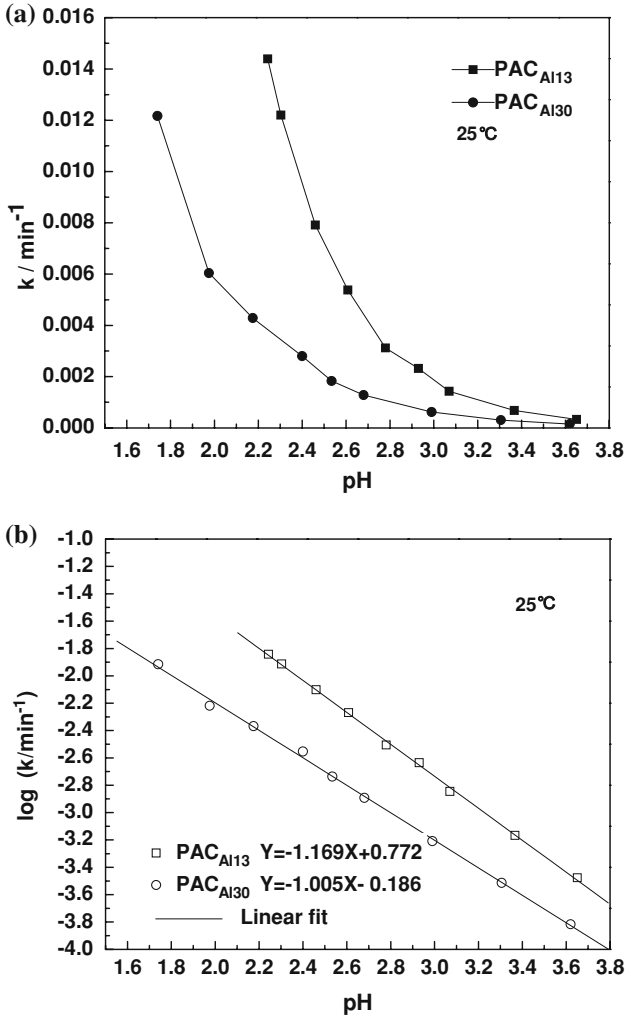

Fig. 4 The decomposition rate constants of Al_{13} and Al_{30} as a function of pH at 25 °C

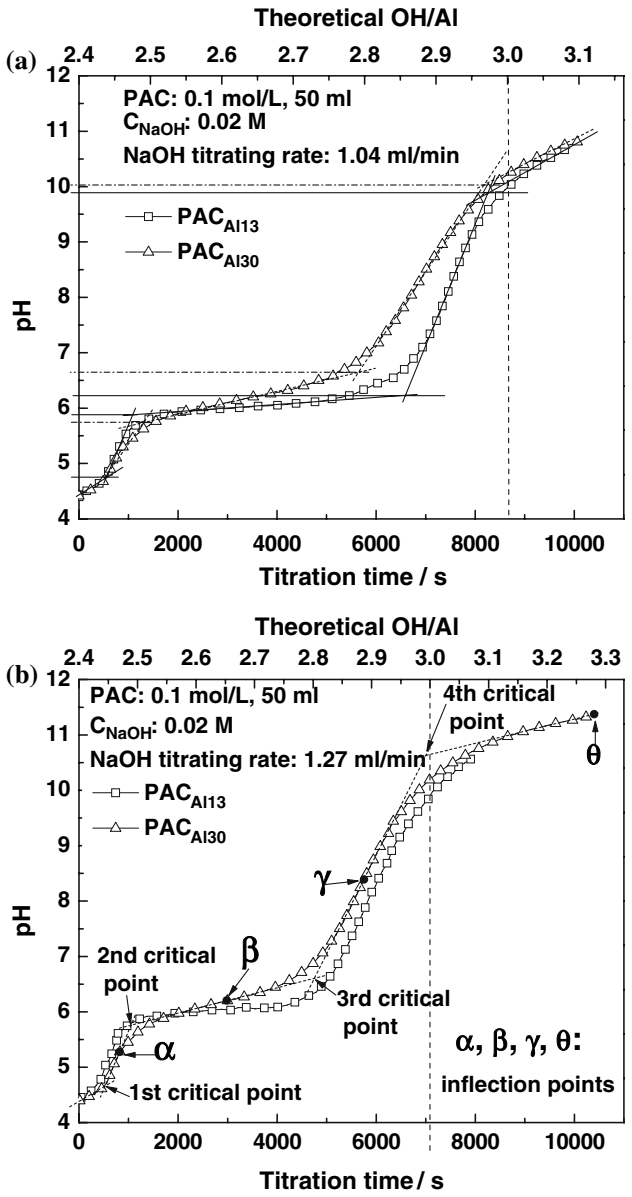

Fig. 5 Titration curves of PAC_{Al13} and PAC_{Al30} with 0.02 M NaOH solution. **a** NaOH solution titrating rate: 1.04 mL/min and **b** NaOH solution titrating rate: 1.27 mL/min

the curve was equal to zero [17]. The changes of characteristic points reflected the transition of deprotonation rate of polymeric Al species under different pH conditions. The titration curves were divided into five districts by the four critical points (Fig. 5). The five districts correspond to five phases of different deprotonation rates (Fig. 6).

As can be seen from Figs. 5 and 6, the solution pH rose slowly for a short time at the beginning of titration. The OH^- added in the first phase were mainly consumed by the hydrolysis and polymerization of Al_{olig} such as $Al(OH)^{2+}$, $Al(OH)_2^{1+}$, $Al_2(OH)_4^{2+}$, etc. Since the amount of these oligomers was small, the titration time was very short. At this phase, the deprotonation number was attributed to the further polymerization of these Al_{olig}.

The pH rose rapidly in the second phase, and the deprotonation number rose slowly. The OH^- added were mainly used to neutralize the free H^+ in solution in this phase. Although the solution pH of PAC_{Al13} and PAC_{Al30} reached 5.9 and 5.75, respectively, the deprotonation numbers of these two coagulants were still small. The corresponding theoretical OH/Al at the second critical point for PAC_{Al13} and PAC_{Al30} were 2.48 and 2.49, respectively. The theoretical OH/Al deducting the OH^- used for elevating the solution pH was about 2.45–2.46, a value which was very close to the OH/Al of Al_{13} molecule. The results further verified that the optimal hydrolysis ratio B for Al_{13} and Al_{30} preparation was about 2.45–2.46. Considering the high Al concentration and local pH

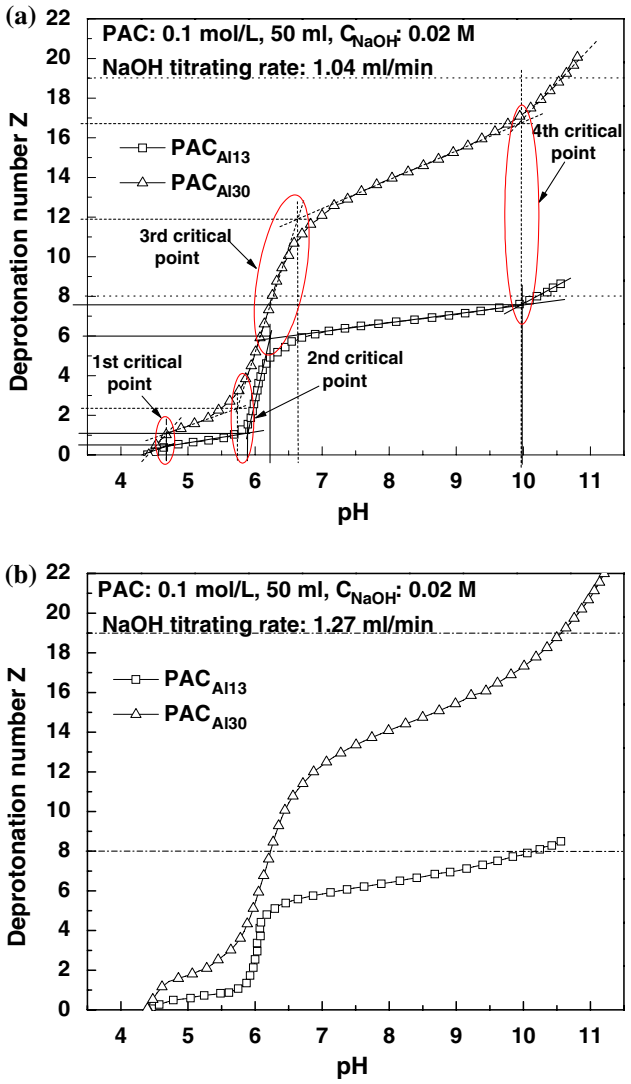

Fig. 6 Plots of calculated deprotonation number Z of Keggin Al_{13} and Al_{30} versus pH. **a** NaOH solution titrating rate: 1.04 mL/min and **b** NaOH solution titrating rate: 1.27 mL/min

gradients caused by drop-wise addition of alkali, we prepared PAC_{Al13} and PAC_{Al30} with $B = 2.4$ in this work.

In the third phase, the pH rose very slowly for a long time, but the deprotonation number increased rapidly in this phase. The OH^- added were mainly used to react with the external coordinated water molecule of Al_{13} and Al_{30}. In this phase, the deprotonation numbers for PAC_{Al13} and PAC_{Al30} were about 5 and 10–11, respectively. Because the deprotonation caused the reduction of charge and the decrease of intra-molecule repulsion, Al_{13} and Al_{30} began to polymerize and aggregate to form soluble $[Al_{13}]_n$ and $[Al_{30}]_n$ aggregates at the second critical point (n denoted the number of Keggin unit). At the third critical point, all Al_{13} and Al_{30} existed in the form of $[Al_{13}]_n$ and $[Al_{30}]_n$ aggregates. The theoretical OH/Al for PAC_{Al13} and PAC_{Al30} in the third phase were 2.48–2.86 and 2.49–2.79, respectively. The theoretical OH/Al ranges were very consistent with the report of Bi et al. [17]. The pH of the third phase ranged 5.9–6.25 and 5.75–6.65 for PAC_{Al13} and PAC_{Al30}, respectively, which indicated that Al_{30} was easier to aggregate than Al_{13} at the acidic side, but $[Al_{13}]_n$ was much easier to convert to sol–gels than $[Al_{30}]_n$. These results are in good agreement with the results of coagulation experiment. Al_{30} was more effective, and had a wider pH usage range than Al_{13} at weak acid side and easier to produce flocs than Al_{13} [27].

In the fourth phase, the solution pH rose rapidly. Part of the OH^- added neutralized the free H^+ in solution, and the other part was used for deprotonation of $[Al_{13}]_n$ and $[Al_{30}]_n$ further. The deprotonation rate became slower relative to the third phase due to the increase of species alkalinity and the steric obstacle of the aggregates. At the fourth critical point, the solution pH for PAC_{Al13} and PAC_{Al30} were 9.9 and 10, with Z reaching 7.5 and 16.8, respectively. Allowing for the deprotonation number of oligomers in the first and second phase, the practical deprotonation numbers of Al_{13} and Al_{30} at the fourth critical point were 6.5 and 15.5, respectively. At pH around 10, the soluble $[Al_{13}]_n$ and $[Al_{30}]_n$ aggregates have completely transformed into sol–gels through deprotonation and polymerization, as well as internal structural adjustment and rearrangement. The sol–gels produced from Al_{13} and Al_{30} were positively charged and thus promote flocculation. The theoretical OH/Al for PAC_{Al13} and PAC_{Al30} at the fourth critical point was lower than 3.0 (Fig. 5). The average hydrolysis ratios of the sol–gels therefore were lower than 3.0, and this explained why the sol–gels possessed positive charges at pH around 10. During the polymerization and gelatination of Al_{13} and Al_{30}, there exist a certain amount of H^+ site in the interior of the aggregates, which could not be neutralized in time due to the steric obstacle and OH^- diffusion limitation. The neutralization hysteresis resulted in the inhomogeneous hydrolysis of Al atom in sol–gels. The hydrolysis ratio B of the internal Al atom inside the clusters was lower than the theoretical OH/Al and contributed mainly to the positive charges of the sol–gels, while the hydrolysis ratio B of the external Al atom was higher than the theoretical OH/Al. The shielding of the external Al atom made the positively charged sol–gels preserved for a long time under high pH condition. The hydrolysis precipitates formed during flocculation were mainly the aggregates of Al_{13} and Al_{30} rather than amorphous $Al(OH)_3$ precipitates.

In the fifth phase, the solution pH rose slowly again. The OH^- added were mainly used to dissolve the sol–gels and this caused the formation of soluble $Al(OH)_4^-$. So the deprotonation rate increased again.

As can be seen from Figs. 5 and 6, the base titration rate had little effect on the pH titration curves and the calculated deprotonation curves. When NaOH titration rate was

increased, the solution pH and theoretical OH/Al of the critical points shifted to slightly high values due to the hysteresis of deprotonation process.

The deprotonation curves of PAC_{Al13} and PAC_{Al30} are shown in Fig. 6. The deprotonation number of PAC_{Al30} was higher than that of PAC_{Al13}, which indicated that Al_{30} aggregated faster than Al_{13}, and correspondingly, the base stability of Al_{30} was weaker than that of Al_{13}. During the second phase, Al_{30} had lost one proton and began to polymerize and aggregate at the pH 4.6–5.75 due to the stronger acidity of the coordinated H_2O of the linked Al atom at the equator, while at the pH 4.75–5.9, Al_{13} species is stable. Most of previous research on polymeric Al species was carried out at Al concentration of about 10^{-3} M, and with this low concentration, the solution pH reached above 5.0. Even though there exists Al_{30} in solution, the Al_{30} could not be detected by ^{27}Al NMR due to the polymerization and aggregation of Al_{30}.

As can be seen from Fig. 6, if the 7 protons on Al_{13} and 18 protons on Al_{30} were neutralized completely (for Al_{13} and Al_{30}, $Z = 8$ and 19, respectively), the solution pH reached 10.2 and 10.5 for Al_{13} and Al_{30}, respectively. Because the aggregation and agglomeration of Al species resulted in the incomplete neutralization of H^+ sites that was located in the interior of aggregates, the pH needed to neutralize the charge or deprive the proton completely was higher than the theoretic values, and it depended on the polymerization degree of Al species. However, the results obtained in this work were very consistent with the charge characteristics of hydrolysis precipitates of PAC_{Al13} and PAC_{Al30} during flocculation [27], and which also explained the flocculation behavior and mechanism of PAC_{Al13} and PAC_{Al30} very well.

Mechanism of stability of Keggin Al_{13} and Al_{30}

Al_{13} and Al_{30} species in polyaluminum coagulants are subjected to medium and high acidic environment ($Al_T = 0.2$–2.5 M, pH = 1.0–4.2) during storage. The schematic diagrams on acid decomposition of Al_{13} and Al_{30} during storage is shown in Scheme 1. The notation and group numbering used here were the same as in Phillips et al. [22] for convenient reference. For Al_{13}, the bridged hydroxyls μ_2-$OH_{(a)}$ are vulnerable to protonation. The protonation of μ_2-$OH_{(a)}$ results in the dissociation of the hydroxyl bridge connecting the four trimeric groups, and which results in the formation of HAl_{13}^{8+}. But the protonation and dissociation of the μ_2-$OH_{(a)}$ are reversible, and the decomposition of Al_{13} could not be achieved until some dissociation of the hydroxyl bridge allow the hydronium to access the center of Keggin and to protonate the μ_4-O groups. The irreversible protonation of μ_4-O groups is the rate-controlling step of the acid decomposition of Al_{13} [38]. The protonation of μ_4-O groups weakens the bonds between AlO_4 and the four external trimeric groups, and which results in the formation of the precursor of $H_2Al_{13}^{9+}$. Further protonation of $H_2Al_{13}^{9+}$ leads to two decomposition pathways: (1) breaking up into Al_m and Al_{olig}, and forming bayerite by recrystallizing the Al_m and Al_{olig}; (2) collapse of the Keggin structure and bayerite formed through structure rearrangement and self-assembly directly. Then bayerite converted to gibbsite ultimately by aging [28].

Based on the oxygen exchange rate between Al_{30} and bulk solution [22], Al–O bond lengths [18, 19], and the relative Brønsted acidities of functional groups [29], the bridged hydroxyls μ_2-$OH_{(3)}$, μ_2-$OH_{(4)}$, and μ_2-$OH_{(5)}$ in Al_{30} were all assumed to be the most possible proton receptor sites. But protonation of μ_2-$OH_{(4)}$ and μ_2-$OH_{(5)}$ is reversible and does not cause the decomposition of Keggin structure. So μ_2-$OH_{(3)}$ is the only hydroxyl site whose dissociation allows the hydronium transferring to μ_4-O groups, and leads to the decomposition of Al_{30} in acid solution. The protonation of μ_4-O in Al_{30} leads to the formation of precursor of $H_2Al_{30}^{+20}$. The precursor decomposed into Al_m, Al_{olig}, and δ-$Al_{(13+i)}$ ($i \leq 7$) when

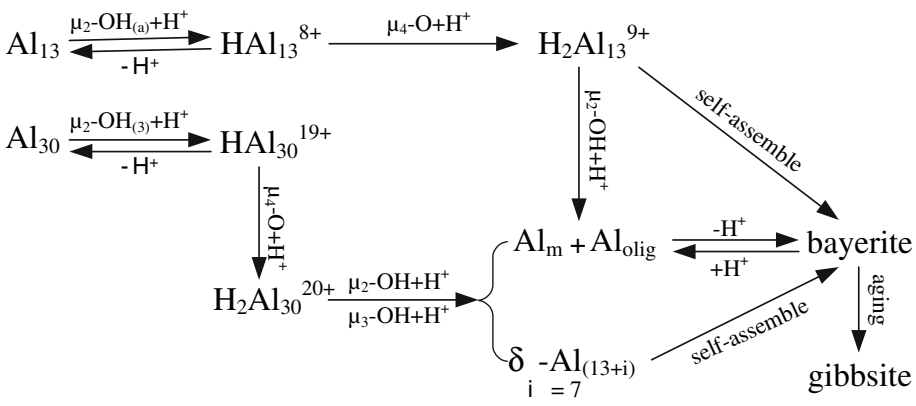

Scheme 1 The schematic diagram on acid decomposition of Al_{13} and Al_{30} during storage

triggered by further protonation other than μ_2-OH and μ_3-OH. Al_m and Al_{olig} then convert to bayerite and gibbsite by re-crystallization and aging. δ-$Al_{(13+i)}$ transforms directly into bayerite through structure rearrangement and self-assembly due to the molecular structure disequilibrium and internal tension.

Compared to Al_{13}, μ_2-$OH_{(2)}$ in Al_{30} are the hydroxyl that connects the four trimeric groups. The dissociation of μ_2-$OH_{(2)}$ did not give way to protonation of μ_4-O groups due to the steric obstacle of the rotated cap trimer. The chance of protonating μ_2-$OH_{(3)}$ in Al_{30} is smaller than that of protonating μ_2-$OH_{(a)}$ in Al_{13} due to the shielding of the adjacent bound waters η-$H_2O_{(3)}$ and η-$H_2O_{(4)}$ in Al_{30}. So, the acid stability of Al_{30} is stronger than that of Al_{13}. It should be pointed out that the protonation decomposition and deprotonation polymerization of Al_{13} and Al_{30} species coexist in polyaluminum coagulant during storage. And the two reacting processes constrain each other by varying the solution pH. But at high acidity conditions, the acid decomposition, and then recrystallization is the dominant process that is responsible for the decrease of Al_{13} and Al_{30} during storage and aging. The deprotonation polymerization will be discussed in following paragraphs.

The schematic diagram on alkaline polymerization of Al_{13} and Al_{30} after dosing into water is shown in Scheme 2. The resulting Al species is closely related to the solution pH. For conventional flocculation process, the solution pH ranges from neutral to weak alkalinity. After dosing into water, the external η-H_2O of Al_{13} and Al_{30} deprotonate rapidly, and Al_{13} and Al_{30} polymerize to $[Al_{13}]_n$ and $[Al_{30}]_n$ clusters. These clusters are composed primarily of repeating Keggin structural units, and grow with a fractal structure. Since the solution pH is higher than the equilibrium pH of $[Al_{13}]_n$ and $[Al_{30}]_n$, these clusters further transform into $Al_{sol-gel}$ with a pseudo-boehmite structure through further deprotonation and internal structure rearrangement. $Al_{sol-gel}$ contains large amounts of AlO_4 tetrahedron, and slowly transform to gibbsite through solid squeezing and structural self-assembly. The coordination number of the tetrahedral Al increases through the cleavage of Al–O–Al bond [39]. The $Al_{sol-gel}$ also can also dissolve by further deprotonation, and forms $Al(OH)_4^-$ in high alkaline solution. Then bayerite forms by protonating the $Al(OH)_4^-$.

Most of positive charges lost during clustering of Al_{13} and Al_{30} and subsequent gelatination of $[Al_{13}]_n$ and $[Al_{30}]_n$ (Scheme 2). Within very narrow pH ranges (5.9–6.25 and 5.75–6.65 for Al_{13} and Al_{30}, respectively), the charges of $[Al_{13}]_n$ and $[Al_{30}]_n$ decreased to +2 and +7–8, respectively. The clustering process is very important to coagulation. In order to give full play to the charge neutralization capacity, Al_{13} and Al_{30} species must interact with the particles in treated water first, and then aggregate and form $[Al_{13}]_n$ and $[Al_{30}]_n$ on particulate surface. Fortunately, the interaction of Al_{13} and Al_{30} with the particles can be promoted by surface catalysis and electrostatic attraction between Al species and particles, because most of particles in treated water are negatively charged, and possess very high specific surface area. The surface reaction involves surface complexation, surface adsorption, and surface precipitation, and which is very beneficial to coagulation. Moreover, $Al_{sol-gel}$ is positively charged at pH 10, and

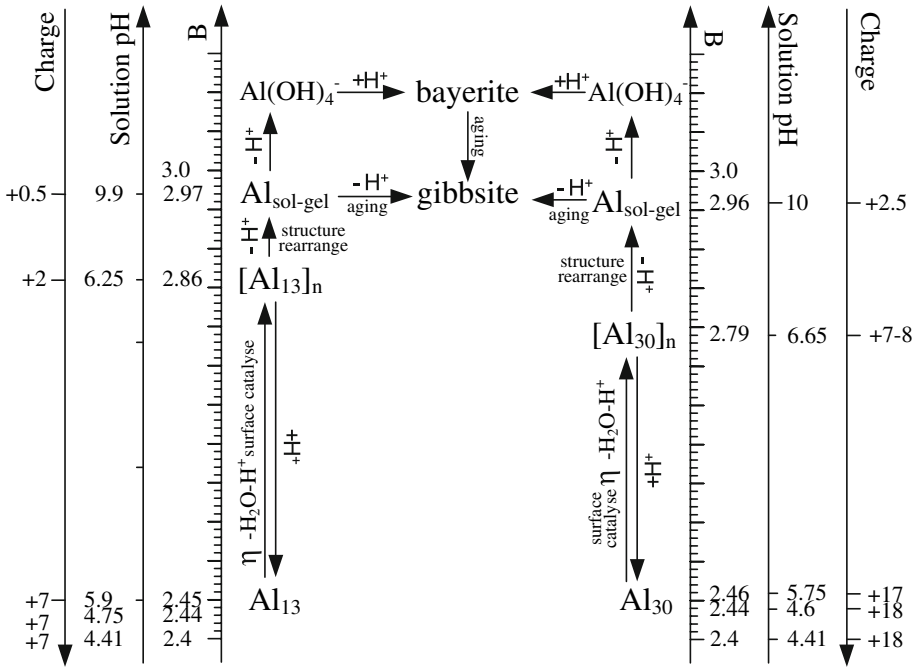

Scheme 2 The schematic diagram on alkaline polymerization of Al_{13} and Al_{30} after dosing, $Al_T = 0.05–0.1$ M

which is very important to coagulation at high pH conditions.

$[Al_{30}]_n$ clusters exist within a wider pH range than $[Al_{13}]_n$, and the polymers derived from Al_{30} possess higher charge than Al_{13}, which demonstrate that Al_{30} possesses better characteristics than Al_{13} when used as coagulant. It should be pointed out that the solution pH and *B* values for Al species transformation shown in Scheme 2 were measured at $Al_T = 0.05$–0.1 M. These values were dependent on the Al_T, and would shift to a lower value when Al_T increased.

Conclusions

The acid catalyzed decomposition and followed by recrystallization is one of the main processes that responsible for the decrease of Al_{13} and Al_{30} in polyaluminum coagulants during storage. The acid decomposition rates of Al_{13} and Al_{30} increased rapidly with the decrease in solution pH. The half-life of Al_{30} was twice longer than that of Al_{13} at 25 °C, and the stability difference increased as the pH decreased. The decomposing reaction orders of Al_{13} and Al_{30} with respect to H^+ concentration are 1.169 and 1.005, respectively. This indicates that the acid decompositions of Al_{13} and Al_{30} are composed of two parallel first-order and second-order reactions. Al_{13} decomposed more rapidly than Al_{30} with the decrease in solution pH due to the higher contribution of the second-order reaction. The effect of temperature on the acid decomposition of the two coagulants was less important than the solution pH. The acid decomposition rates of Al_{13} and Al_{30} increased slightly as temperature increased from 20 °C to *ca.* 35 °C, but decreased when temperature increased further because of the exothermic character of the first-order reaction. The high Al_T, high temperature, and long-term thermal treatment promoted Al_{13} converting to Al_{30} during commercial polyaluminum coagulants preparation, and at the same time, Al_{30} was more stable than Al_{13} upon acid decomposition during the storage of coagulants. So, Al_{30} is more possible to become the dominant species in polyaluminum coagulants than Al_{13}, and the results also provide a reasonable interpretation on why Al_{13} content is low in polyaluminum commercial coagulants.

Al_{13} and Al_{30} in polyaluminum coagulants deprotonate and polymerize rapidly during flocculation process, and form clusters of $[Al_{13}]_n$ and $[Al_{30}]_n$ with repeating Keggin structural units. The clusters further transform into $Al_{sol-gel}$ with a pseudo-boehmite structure through further deprotonation and internal structure rearrangement. $Al_{sol-gel}$ slowly transforms to gibbsite through solid squeezing and structural self-assembly, or converts to bayerite and gibbsite via $Al(OH)_4^-$. The hydrolysis products depend on solution pH. The fresh hydrolysis precipitates formed at $pH \geq 7$ are positively charged, and consist mainly of repeating Al_{13} and Al_{30} units rather than amorphous $Al(OH)_3$ precipitates. $[Al_{13}]_n$ and $[Al_{30}]_n$ have +2 and +7–8 positive charges, respectively, and $Al_{sol-gel}$ derived from Al_{13} and Al_{30} possess +0.5 and +2.5 positive charges, respectively. The positively charged clusters and sol–gels are beneficial to the flocculation. The stability of Al_{30} is lower than that of Al_{13} upon alkaline hydrolysis. Al_{13} maintains stable at $pH < 5.9$, while Al_{30} has lost one proton at the pH 4.6–5.75 due to the strong acidity of η-$H_2O_{(3)}$ and η-$H_2O_{(4)}$ at the equator of Al_{30}. Al_{13} loses 5 protons within the pH range of 5.9–6.25, and Al_{30} loses 10 protons within the pH range of 5.75–6.65. Al_{30} is easier to aggregate than Al_{13} at the acidic side, while $[Al_{13}]_n$ is much easier to convert to sol–gels than $[Al_{30}]_n$. Al_{30} possesses better characteristics than Al_{13} when used as coagulant because $[Al_{30}]_n$ clusters exist at a wider pH range, and the alkaline hydrolysis products of Al_{30} possess higher charges than that of Al_{13}. The results are very consistent with the results of flocculation experiments, and which can explain the flocculation behavior and mechanism of Al_{13} and Al_{30} very well.

Acknowledgements The work was financially supported by the National High Technology Research and Development Key Program of China (863 Program) (No. 2002AA601290) and the National Natural Science Foundation of China (No. 50874098 and No. 40673003).

Appendix

Al_{30} and Al_{13} are decomposed by H^+ in the continuous flow reactor. It is assumed that Al_{30} species added into the reactor exists in two extreme states: keeping Al_{30} species or decomposing completely into Al^{3+} by H^+ according to the following stoichiometry:

$$[Al_2O_8Al_{28}(OH)_{56}(H_2O)_{24}]^{18+} + 72H^+ \rightarrow 30Al^{3+} + 88H_2O. \quad (4)$$

It is assumed that the above acid decomposition reaction is a pseudo-first-order reaction with respect to Al_{30}, and the decomposition rate described as:

$$r = k_{Al_{30}} \cdot [Al_{30}]. \quad (5)$$

$k_{Al_{30}}$ is the apparent rate coefficient of the pseudo-first-order reaction calculated by Al_{30} concentration (min^{-1}); $[Al_{30}]$ is the concentration of Al_{30} in reactor (M).

It is assumed that the solution in the reactor is fully mixed and homogeneous, and the concentrations of Al_{30} and H^+ in

the outflow are equal to that in the reactor. The mass balance equations of Al_{30} and H^+ in continuous flow reactor are:

$$\frac{d[Al_{30}]}{dt} = \frac{V_{Al_{30}} \cdot [Al_{30}]_{in} - (V_{Al_{30}} + V_{HCl}) \cdot [Al_{30}]}{V_r} - k_{Al_{30}} \cdot [Al_{30}] \quad (6)$$

and

$$\frac{d[H^+]}{dt} = \frac{V_{HCl} \cdot [HCl]_{in} - (V_{Al_{30}} + V_{HCl}) \cdot [H^+]}{V_r} - 72k_{Al_{30}} \cdot [Al_{30}]. \quad (7)$$

$V_{Al_{30}}$ and V_{HCl} are the volume flow rates of PAC_{Al30} and hydrochloric acid that added into the reactor, respectively (L/min); V_r denotes the volume of solution in the reactor (L); $[Al_{30}]_{in} = Al_T/30$ and $[HCl]_{in}$ are the concentration of Al_{30} and hydrochloric acid that are added into the reactor, respectively (M).

The concentrations of Al_{30} and H^+ in the reactor remain constant at the stable state,

$$\frac{d[Al_{30}]}{dt} = 0 \quad (8)$$

$$\frac{d[H^+]}{dt} = 0. \quad (9)$$

From Eqs. (6)–(9), the following expressions are derived:

$$k_{Al_{30}} = \frac{V_{HCl} \cdot (V_{Al_{30}} + V_{HCl}) \cdot [HCl]_{in} - (V_{Al_{30}} + V_{HCl})^2 \cdot [H^+]_{stat}}{72V_{Al_{30}} \cdot V_r \cdot [Al_{30}]_{in} + V_r \cdot (V_{Al_{30}} + V_{HCl}) \cdot [H^+]_{stat} - V_r \cdot V_{HCl} \cdot [HCl]_{in}}, \quad (10)$$

$$[Al_{30}]_{stat} = \frac{30V_{Al_{30}} \cdot [Al_{30}]_{in}}{V_r \cdot k_{Al_{30}} + V_{Al_{30}} \cdot (V_{Al_{30}} + V_{HCl})}. \quad (11)$$

$[Al_{30}]_{stat}$ and $[H^+]_{stat}$ denote the concentration of Al_{30} (calculated by Al) and H^+ in the reactor at stable state, respectively (M).

The half-life ($t_{1/2}$, min) of pseudo-first-order reaction of acid decomposition of Al_{30} is calculated by the following equation:

$$t_{1/2} = \frac{LN(2)}{k_{Al_{30}}}. \quad (12)$$

For Al_{13}, the acid decomposition stoichiometric equation is:

$$[AlO_4Al_{12}(OH)_{24}(H_2O)_{12}]^{7+} + 32H^+ \rightarrow 13Al^{3+} + 44H_2O. \quad (13)$$

The following equations are obtained according to the same calculation methods as described above:

$$k_{Al_{13}} = \frac{V_{HCl} \cdot (V_{Al_{13}} + V_{HCl}) \cdot [HCl]_{in} - (V_{Al_{13}} + V_{HCl})^2 \cdot [H^+]_{stat}}{32V_{Al_{13}} \cdot V_r \cdot [Al_{13}]_{in} + V_r \cdot (V_{Al_{13}} + V_{HCl}) \cdot [H^+]_{stat} - V_r \cdot V_{HCl} \cdot [HCl]_{in}}, \quad (14)$$

$$[Al_{13}]_{stat} = \frac{13V_{Al_{13}} \cdot [Al_{13}]_{in}}{V_r \cdot k_{Al_{13}} + V_{Al_{13}} \cdot (V_{Al_{13}} + V_{HCl})}, \quad (15)$$

$$t_{1/2} = \frac{LN(2)}{k_{Al_{13}}}. \quad (16)$$

$[Al_{13}]_{stat}$ is the concentration of Al_{13} (calculated by Al) in the reactor at steady state (M). $k_{Al_{13}}$ is the apparent rate coefficient of the pseudo-first-order reaction calculated by Al_{13} concentration (min^{-1}); $[Al_{13}]_{in} = Al_T/13$ and $V_{Al_{13}}$ are the Al_{13} concentration and volume flow rate of PAC_{Al13} that are added into the reactor (M and L/min, respectively).

References

1. Bertsch PM, Parker DR (1996) In: Sposito G (ed) The environmental chemistry of aluminum. CRC Press, New York, p 117
2. Jolivet JP, Henry M, Livage J (2000) Metal oxide chemistry and synthesis from solution to solid state. Wiley, Chichester, p 53

3. Casey WH, Phillips BL, Furrer G (2001) In: Banfield JF, Navrotsky A (eds) Nanoparticles and the environment, Reviews in Mineralogy & Geochemistry, vol 44. Mineralogical Society of America and Geochemical Society, Washington, DC, p 167
4. Duan JM, Gregory J (2003) Adv Colloid Interface Sci 100–102:475
5. Pernitsky DJ (2001) Drinking water coagulation with polyaluminum coagulants—mechanism and selection guidelines. PhD thesis, University of Massachusetts
6. Aceman S, Lahav N, Yariv S (2000) Appl Clay Sci 17:99
7. Occelli ML, Bertrand JA, Gould SAC, Dominguez JM (2000) Micropor Mesopor Mater 34:195
8. Ahmad MHARM, Mahmood CS, Mohamed AA, Ibrahim A, Alias R, Shapee SM, Yahya MR, Mat AFA (2008) Mater Lett 62:2339
9. Wang M, Muhammed M (1999) Nanostruct Mater 11:1219
10. Fitzgerald JJ (1988) In: Laden K, Felger C (eds) Antiperspirants and deodorants. Dekker, New York, p P119
11. Casey WH, Rustad JR, Banerjee D, Furrer G (2005) J Nanopart Res 7:377
12. Phillips BL, Casey WH, Karlsson M (2000) Nature 404:379
13. Furrer G, Phillips BL, Ulrich KU, Pöthig R, Casey WH (2002) Science 297:2245
14. Hunter D, Ross DS (1991) Science 251:1056
15. Parker DR, Bertsch PM (1992) Environ Sci Technol 26:914
16. Tang HX (1998) Acta Sci Circumst 18:1 in Chinese
17. Bi SP, Wang CY, Cao Q, Zhang CH (2004) Coord Chem Rev 248:441
18. Allouche L, Gérardin C, Loiseau T, Férey G, Taulelle F (2000) Angew Chem Int Ed 39:511
19. Rowsell J, Nazar LF (2000) J Am Chem Soc 122:3777
20. Seichter W, Mögel HJ, Brand P, Salah D (1998) Eur J Inorg Chem 6:795
21. Casey WH, Olmstead MM, Phillips BL (2005) Inorg Chem 44:4888
22. Phillips BL, Lee A, Casey WH (2003) Geochim Cosmochim Acta 67:2725
23. Allouche L, Huguenard C, Taulelle F (2001) J Phys Chem Solids 62:1525
24. Allouche L, Taulelle F (2003) Inorg Chem Commun 6:1167
25. Shafran KL, Deschaume O, Perry CC (2005) J Mater Chem 15:3415
26. Shafran KL, Perry CC (2005) Dalton Trans 2098
27. Chen ZY, Fan B, Peng XJ, Zhang ZG, Fan JH, Luan ZK (2006) Chemosphere 64:912
28. Chen ZY, Luan ZK, Fan JH, Zhang ZG, Peng XJ, Fan B (2007) Coll Surf A Physicochem Eng Aspects 292:110
29. Rustad JR (2005) Geochim Cosmochim Acta 69:4397
30. Gao BY, Yue QY, Wang BJ (2002) Chemosphere 46:809
31. Wang WZ, Hsu PH (1994) Clay Clay Miner 42:356
32. Chen ZY, Liu CJ, Luan ZK, Zhang ZG, Li YZ, Jia ZP (2005) Chin Sci Bull 50:2010
33. Furrer G, Gfeller M, Wehrli B (1999) Geochim Cosmochim Acta 63:3069
34. Furrer G, Ludwig C, Schindler PW (1992) J Coll Interf Sci 149:56
35. Lee AP, Furrer G, Casey WH (2002) J Coll Interf Sci 250:269
36. Parker DR, Bertsch PM (1992) Environ Sci Technol 26:908
37. Chen ZY, Luan ZK, Fan B, Zhang ZG, Li YZ, Jia ZP (2006) Chin J Anal Chem 34:38 in Chinese
38. Casey WH, Phillips BL, Karlsson M, Nordin S, Nordin JP, Sullivan DJ, Susan NC (2000) Geochim Cosmochim Acta 64:2951
39. Bradley SM, Kydd RA, Howe RF (1993) J Coll Interf Sci 159:405